

Hydro-Bio-Mechanical Model: Overview .....	155
CONCEPTUAL FRAMEWORK .....	155
IMPLEMENTATION.....	156
THEORY INTO PRACTICE: VERIFICATION AND VALIDATION .....	157
 Hydraulic Model .....	 159
PARAMETER REQUIREMENTS .....	159
UNSATURATED FLOW .....	159
Moisture retention.....	160
Moisture retention or absorptive capacity? .....	163
MOISTURE FLOW & HYDRAULIC CONDUCTIVITY .....	164
Phase-dependent saturated hydraulic conductivity.....	164
 Biodegradation Model .....	 168
PARAMETER REQUIREMENTS .....	168
MINERALISATION .....	168
Metabolic pathway.....	168
Kinetics of enzymatic hydrolysis.....	169
<i>Digestibility</i> .....	170
<i>Product inhibition</i> .....	170
<i>Maximum rate of hydrolysis</i> .....	171
<i>Moisture content</i> .....	171
<i>Modified functional form</i> .....	172
Methanogenesis .....	172
Transport, growth and decay - governing equations.....	174
Substrate depletion .....	174
Moisture consumption .....	175
 Mechanical Model .....	 177
PARAMETER REQUIREMENTS .....	177
LANDFILL SETTLEMENT .....	178
Load-induced behaviour - Elasto-plasticity .....	178

---

<i>Elastoplasticity: key features</i> .....	179
Creep behaviour - Visco-elasto-plasticity.....	180
Biodegradation-induced settlement: Bio-plasticity .....	183
PARAMETER ESTIMATION – LABORATORY TESTS.....	185
Initial conditions .....	188
HYDRAULIC VARIABLES.....	188
BIODEGRADATION VARIABLES.....	188
VFA.....	188
Methanogenic biomass .....	188
Link Routines .....	190
HYDRAULIC-BIODEGRADATION (HB) LINK .....	190
BIODEGRADATION-MECHANICAL (BM) LINK .....	190
MECHANICAL-HYDRAULIC (MH) LINK.....	190
Element types .....	191
Numerical control.....	192
References .....	194
Appendix 1      Summary of HBM Parameters .....	197

## Hydro-Bio-Mechanical Model: Overview

### CONCEPTUAL FRAMEWORK

The HBM model provides a framework for the integrated analysis of the hydraulic, biodegradation and mechanical behaviour of landfilled waste or other degradable soils.

Building on individually-proven models of hydraulic, biodegradation and mechanical behaviour, the HBM model gives a synergistic interpretation of landfill behaviour with relatively light input parameter requirements.

The HBM model comprises three main system models and link routines, through which the algorithm passes, as shown in Fig.1. It is in the link routines that the most recent system variable values are used to update the conditions within each system model.

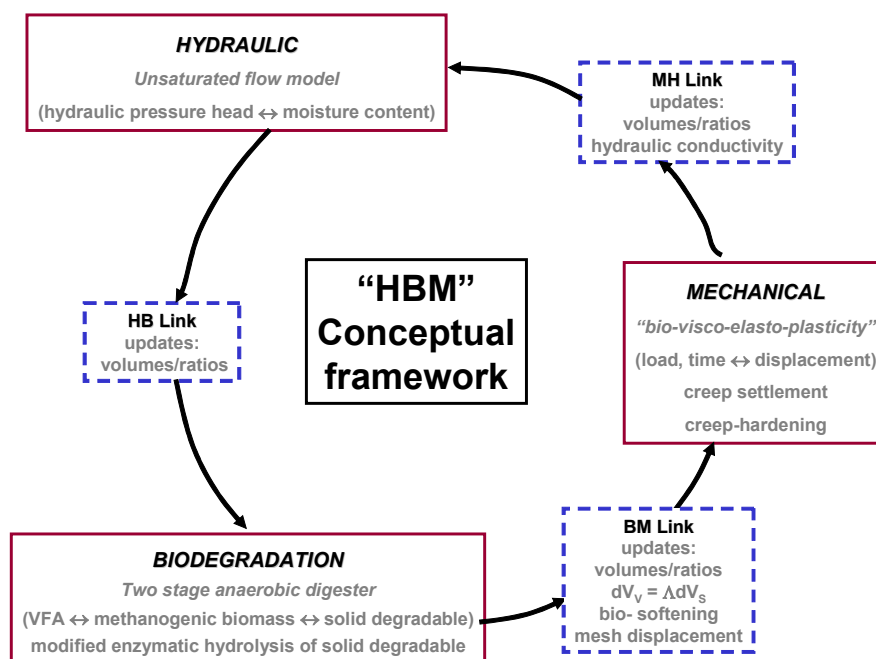
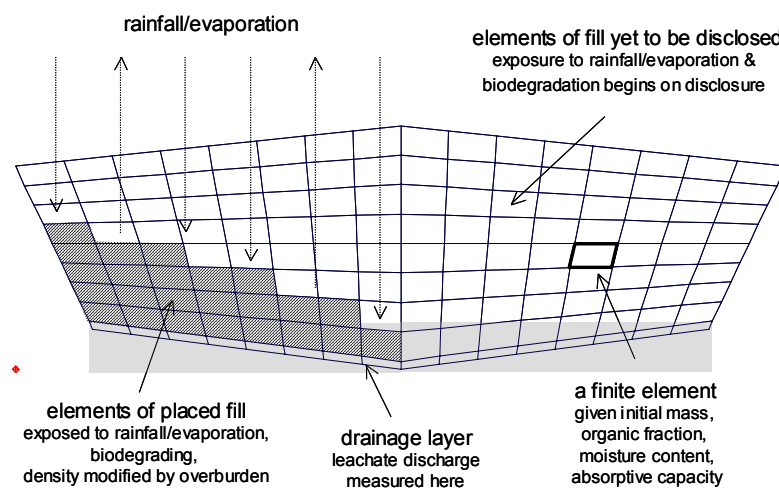


Figure 1 Schematic representation of the HBM conceptual framework.

## IMPLEMENTATION

The HBM model is implemented using the finite element method, with each system model sharing a common mesh. Using this method it is possible to account for material and operational features such as complex section geometry, waste heterogeneity, anisotropic hydraulic conductivity and simulation of the filling phase.

Operation of the HBM model, i.e. preparation of simulation input data and interrogation of output data, is through the graphical user interface – HBM GUI.

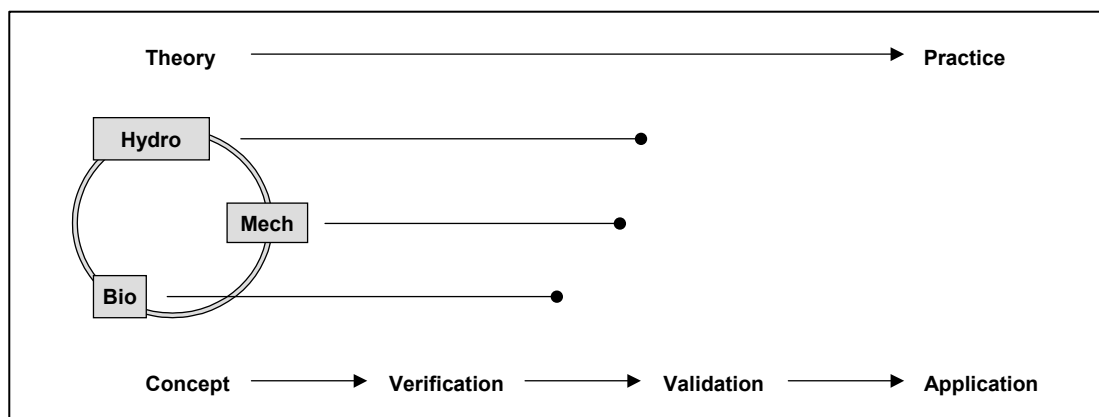


**Figure 2 Finite element mesh illustrating filling.**

## THEORY INTO PRACTICE: VERIFICATION AND VALIDATION

The Examples Manual covers seven distinct landfill scenarios; with minor adjustments, 14 simulations are presented. The simulations have been chosen to elucidate the potential of the HBM model. They also reveal the model's journey from theory into practice, which, because of the combination of three component system models, cannot be simply summarised.

As isolated system models, the hydraulic and mechanical models are close to practice, actually the basis of well established design tools. However, in the HBM framework each system model can modify parameters in other systems. These system interdependencies are the innovative aspect of the HBM model. They are less well understood and have necessitated a fundamental review of the performance of the combined framework. An indication of the individual model development within the context of the HBM framework is given in Fig. 3.



The table adds some substance to the state of model development in isolation and the interdependencies within HBM framework. There are significant challenges in the interdependencies; for example, the mechanical consequences of decomposition have until now, received little attention in either the landfill or geotechnical research communities. But the rewards are great. If the interdependencies can be sensibly understood, then hitherto disparate behaviours can be analysed in a much more meaningful and coherent context.

**Figure 3 Progress of HBM model from theory to practice**

Systems	Interpretation/Interdependence		
	Hydraulic	Biodegradation	Mechanical
<b>Hydraulic</b>	Long history of unsaturated flow modelling. Commercial software available.	Advective flux commonly incorporated	Impact of moisture / suction on compressibility or strength unknown
<b>Biodegradation</b>	Few hydro-biodegradation models where moisture is limited and consumed as reactant.	Long history of two-stage anaerobic digestion modelling. HBM uses moisture dependent enzymatic cellulolytic hydrolysis	Few studies of impact of decomposition on mechanical behaviour. HBM introduces decomposition-induced void change.
<b>Mechanical</b>	Void phase controls permeability but little knowledge of decomposition effects.	Responds to changing phase composition	Well-established legacy of mechanical modelling in unsaturated soils. Commercial software available.

## Hydraulic Model

The hydraulic model is an unsaturated flow model in which the main system variables are hydraulic pressure head and moisture content.

### PARAMETER REQUIREMENTS

Parameter requirements are given in the table below; justification for the selection of hydraulic parameter values are given in the relevant sections.

	Input parameter	Dimensions	Waste
<b>Hydraulic</b>			
H1	Van Genuchten $\alpha$		1.4
H2	Van Genuchten $n$		1.6
H3	Residual moisture content (w/w)		0.25
H4	Specific storage		0
H5	Saturated hydraulic conductivity	m.s <sup>-1</sup>	5x10 <sup>-5</sup>
H6	Ratio: vert. to horiz. conductivity		1

### UNSATURATED FLOW

Moisture content in volumetric form is denoted by  $\theta$

$$1] \quad \theta = \frac{V_W}{V_T}$$

where  $V_W$  is volume of water and  $V_T$  is total volume.

The hydraulic head  $h$ , is made up of a hydraulic pressure head  $\psi$ , and an elevation head  $z$ , i.e.,

$$2] \quad h = \psi + z$$

The hydraulic pressure head in this form is well known to geotechnical engineers and others; it is based on gauge pressure, thus, at atmospheric pressure  $\psi = 0$  m. In a saturated zone below a phreatic surface, or water table, the value of  $\psi$  is positive; above a phreatic surface, in the vadose or unsaturated zone, the value of  $\psi$  is negative.

Under hydrostatic conditions, there is no flow so  $h$  is uniform throughout the flow domain.

### Moisture retention

It is a fundamental feature of unsaturated soil behaviour that the moisture retained in a porous medium is a function of the applied hydraulic pressure head or suction. This suction–moisture content relationship is required for the solution of unsaturated flow problems. In the HBM model, the relationship is defined using van Genuchten's (1980) expression,

$$3] \quad \theta = \theta_r + \frac{(\theta_s - \theta_r)}{\left[1 + (\alpha|\psi|)^n\right]^m}$$

where the absolute value of  $\psi$  is used,  $\theta_r$  and  $\theta_s$  are the residual and saturated volumetric moisture contents respectively;  $\alpha$ ,  $n$  and  $m$  are model parameters. Figure 4 shows a moisture retention curve, effectively the equilibrium moisture profile, with the meaning of the van Genuchten parameters highlighted.

Parameter  $m$  has no physical interpretation and is often fixed as a function of  $n$ ,

$$4] \quad m = 1 - \frac{1}{n}$$

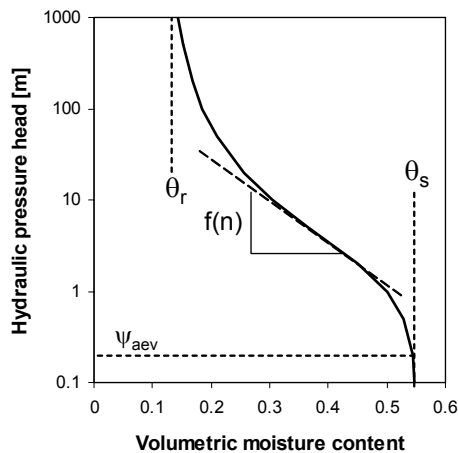


**Figure 4 Moisture retention curve showing meaning of van Genuchten parameters.**

Values for parameters  $\alpha$  &  $n$  have been obtained from laboratory tests reported by Kazimoglu et al, 2005. Figure 5 shows the retention curve with the corresponding retention curve parameters enumerated in the table.

Volumetric moisture contents are physical soil properties. The residual moisture content is the moisture content below which little change in moisture content occurs, regardless of the applied pressure head. It is defined in the HBM model as a gravimetric moisture content of the contemporaneous solid mass.

Values for the gravimetric residual moisture content have been based on neutron probe data obtained by Yuen (1999) from the Lyndhurst Sanitary Landfill in Victoria, Australia. Fig. 6 shows that the upper elevations (0-4m) of the 12 m deep landfill have reached a relatively uniform gravimetric moisture content of about 25%, which we have taken to be the residual condition.

Parameter	Value
$\theta_R$	0.14
$\theta_s$	0.58
A	1.5
N	1.60

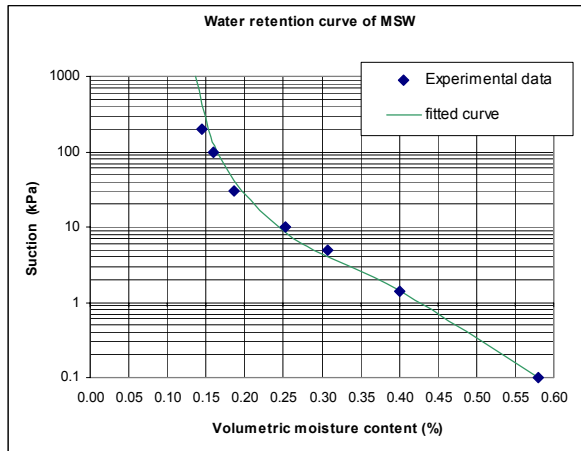


**Figure 5: Moisture retention curve of compacted waste sample obtained using modified pressure plate apparatus, from Kazimoglu et al (2005).**

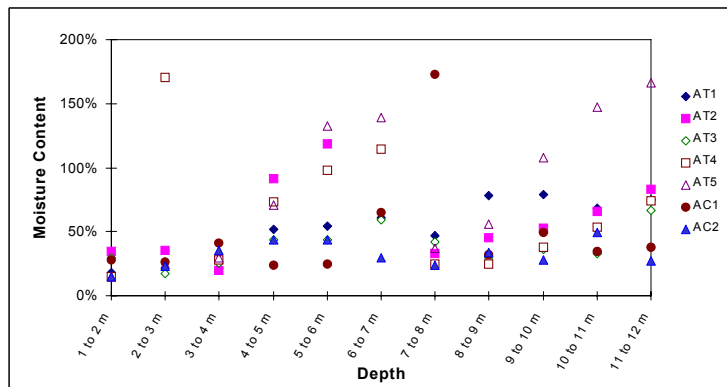


**Figure 6: Profile of gravimetric moisture content in waste at Lyndhurst Sanitary Landfill (Yuen, 1999)**

The saturated moisture content is strictly equivalent to the porosity of the porous medium, which is calculated by the HBM model from contemporaneous mass and unit weight data. In practice, the presence of occluded air means fully saturated moisture content is unlikely to be reached. Values of 90% or less are typical of the maximum degree of saturation especially after cycles of drying and wetting. In waste refuse, saturation levels may be even lower due to the production of landfill gas.

### Moisture retention or absorptive capacity?

Consider the placement of an element of waste of known initial volumetric moisture content ( $\theta = 0.33$ ) in a landfill with an equilibrium moisture profile corresponding to that shown in Figure 7. If the waste is placed near the bottom of the landfill its equilibrium moisture content exceeds the as-placed value and it has the capacity to absorb moisture. In contrast, the same waste placed at the top of a landfill has a moisture content that exceeds the equilibrium condition. Moisture will therefore drain to lower levels. The inescapable conclusion of this interpretation is that absorptive capacity is not a simple constant but is dependent on position within the waste pile. Of course this rationale is usually masked by the heterogeneity of landfilled waste and no account has been taken of compression in the lower layers. From a practical point of view, knowledge of the moisture retention properties avoids the need to define absorptive capacity and provides for a more fundamental interpretation of moisture retention and discharge in relation to prescribed rainfall and filling patterns.

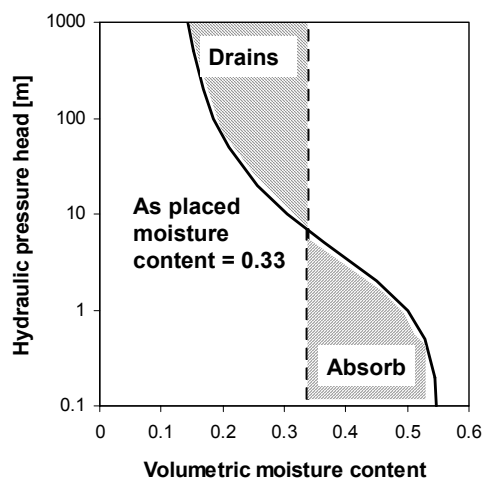


**Figure 7 Placement of waste of fixed moisture content, moisture retention and redistribution**

## MOISTURE FLOW & HYDRAULIC CONDUCTIVITY

Moisture flow is driven by a hydraulic head gradient and assumed to comply with Darcy's Law. In unsaturated zones the coefficient of permeability or hydraulic conductivity  $k(\theta)$ , is dependent on the amount of moisture,

$$5] \quad k(\theta) = k_{sat} k_r$$

where  $k_{sat}$  is the saturated hydraulic conductivity and  $k_r$  is the relative permeability.

The saturated hydraulic conductivity of waste has been reported on by many workers and is generally acknowledged to have a wide range of values. For the purposes of the initial example simulations a waste saturated hydraulic conductivity of  $5 \times 10^{-5}$  m/s has been adopted. More realistic interpretations of conductivity, based on the volumetric state of the waste, are dealt with in the next section.

The relative permeability, which is a function of the moisture saturation, is defined using van Genuchten's (1980) function.

$$6] \quad k_r(\theta) = \sqrt{\theta_e} \left[ 1 - \left( 1 - \theta_e^{1/m} \right)^m \right]^2$$

where  $\theta_e$  is the effective moisture content.

### Phase-dependent saturated hydraulic conductivity

It is known that the saturated hydraulic conductivities of a sample of waste can vary by three or more orders of magnitude when compressed over the range of stresses exerted within 20m depth of waste (Powrie et al., 1998). The HBM model can determine the saturated hydraulic conductivity from the volumetric state of each element. A relationship between saturated hydraulic conductivity and the void volume, expressed as a ratio of the solid inert phase volume is used. In this way, a simple interpretation of the influence of decomposition, through its impact on void volume, is also realised.

From data obtained by Beaven (2000) on the saturated hydraulic conductivity of household wastes in a large (2m dia x 2m high) compression cell, it is evident that the relationship between dry unit weight and saturated hydraulic conductivity can be described by a function of the form,

$$7] \quad k_{sat} = B \exp(c \cdot \gamma_d)$$

where  $\gamma_d$  is the dry unit weight, B and c are fitting parameters. From Fig. 8, we might assume approximate values for DM3 of B = 0.15 and c = -2.0. However, in a degrading soil comprising inert and degradable solid phases, which have different phase densities (or specific gravities), the overall dry unit weight can correspond to more than one volumetric state.

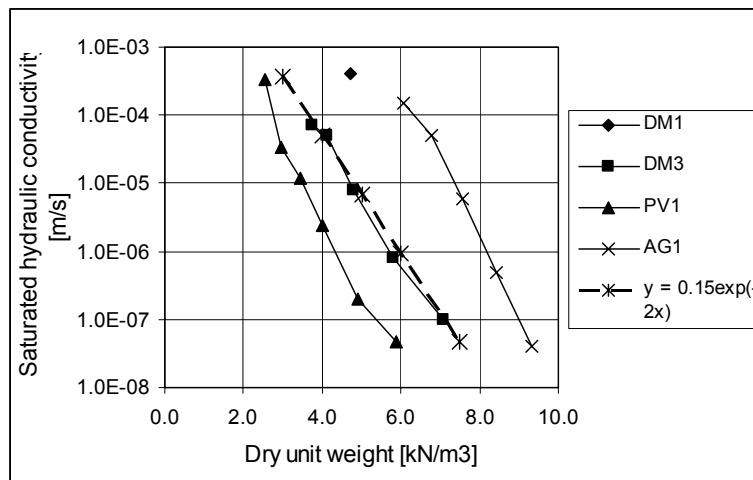


**Figure 8. Variation of saturated hydraulic conductivity with dry unit weight, from data published by Beaven (2000).**

A more useful controlling variable would be the void to inert ratio,  $e_i$ , given by,

$$8] \quad e_i = \frac{V_V}{V_{SI}}$$

where  $V_V$  is the void volume and  $V_{SI}$  is the solid inert phase volume (McDougall & Pyrah, 2004). Equation [8] can be expanded to define  $e_i$  in relation to a simple waste classification and dry unit weight,

$$9] \quad e_i = \frac{G_{SI} \cdot \gamma_w}{\gamma_d (1 - \omega)} - \frac{G_{SI} \cdot \gamma_w \cdot \omega}{G_{SD} \cdot \gamma_w \cdot (1 - \omega)} - 1$$

where  $G_{SI}$  is the specific gravity of the inert phase component,  $G_{SD}$  is the specific gravity of the degradable phase component,  $\gamma_w$  is the unit weight of water and  $\omega$  is the mass fraction of solid degradable matter as a proportion of total solid mass.

Data from Figure 8 can then be re-interpreted as a function of  $e_i$ . Figure 9 shows the DM3 conductivity data in this context, assuming<sup>1</sup> the solid degradable dry weight fraction of sample DM3 is 0.54 and the phase weights of the inert phase  $G_{SI} \cdot \gamma_w = 17 \text{ kN/m}^3$  and degradable phase  $G_{SD} \cdot \gamma_w = 7.3 \text{ kN/m}^3$ . The fitted function is logarithmic in form,

$$10] \quad k_{sat} = 1.0e^{-8} x(e_i)^{4.9}$$

Equation [10] is currently hard-coded into the HBM model.

---

<sup>1</sup> Data presented by Beaven (2000) shows wet weight composition of DM3 to comprise:

- Paper & Card, Garden food & Misc Combustibles, Textile = 70.3 (degradable)
- Plastic, Glass, Metal, Misc non-combustibles = 29.7 (inert)

As a rough guide, wet unit weights of the degradable components are double the dry unit weights, whereas the wet and dry unit weights of the inert components are about the same, we can assume the solid degradable fraction by dry weight is  $35.15/64.85 = 0.54$ . For more information on the compositional analysis see McDougall, Pyrah & Yuen (2004).

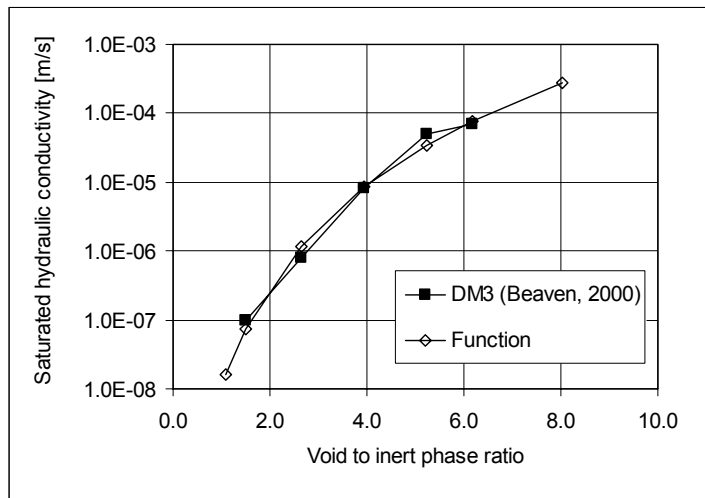


**Figure 9. Waste saturated hydraulic conductivity data (DM3 from Beaven, 2000) presented as a function of void to inert phase ratio**

One should be aware, however, that these bulk saturated hydraulic conductivities may not be representative of field conditions. The influence of low conductivity pathways or channels, which enable leachate to travel through the waste mass in shorter times than would be predicted using experimentally derived bulk conductivity parameters, should be recognised. However, if channelling were to be depicted within a continuum approach to moisture flow, then higher saturated hydraulic conductivities will serve to moderate the prominence of distinct wetting fronts and thereby have a positive effect on flux reporting accuracy.

## Biodegradation Model

The biodegradation model describes a two-stage anaerobic digester in which total volatile fatty acid (VFA) and methanogenic biomass (MB) concentrations are the main field variables controlling mineralisation of organic matter. Solid degradable fraction (SDF) depletion is also an unknown and is the principal output of the biodegradation model.

### PARAMETER REQUIREMENTS

Parameter requirements are given in the table; justification for the selection of biodegradation parameter values are given in the relevant sections.

	Input parameter	Dimensions	Waste
<b>Biodegradation</b>			
B1	Maximum hydrolysis rate	$\text{g.m}^{-3}_{(\text{aq})}.\text{day}^{-1}$	2500
B2	Product inhibition	$\text{m}^3.\text{g}^{-1}$	$2 \times 10^{-4}$
B2	Digestibility		0.7
B3	Half rate	$\text{g.m}^{-3}$	4000
B5	Methanogen growth	$\text{day}^{-1}$	0.02
B6	Methanogen death	$\text{day}^{-1}$	0.002
B7	Yield coefficient		0.08
B8	Diffusion coefficient	$\text{m}^2.\text{day}^{-1}$	0.05
I1	Initial solid degradable fraction		0.4
I2	Initial VFA concentration	$\text{g.m}^{-3}$	300
I3	Initial methanogenic biomass	$\text{g.m}^{-3}$	250

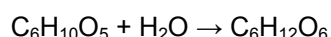
### MINERALISATION

#### Metabolic pathway

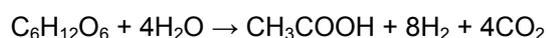
The mineralisation of organic matter is a microbially mediated process, dependent on the nature of the substrate and environmental conditions such as availability of moisture.

Because of the large amount of cellulolytic matter present in the organic fraction of municipal waste, mineralization is here defined by a metabolic pathway of the kind commonly associated with the anaerobic digestion of cellulose. The process is idealised by three main steps:

1. Enzymatic hydrolysis of solid cellulose ( $C_6H_{10}O_5$ ) to glucose ( $C_6H_{12}O_6$ ).

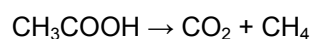


2. Fermentation of glucose to acetic acid ( $CH_3COOH$ ).

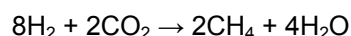


3. Methanogenesis,

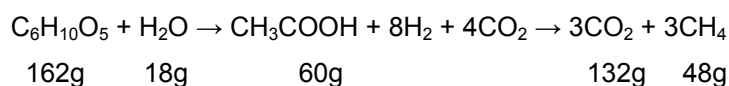
- i) by acetate cleavage



- ii) by hydrogen-scavenging bacteria.



Given the relative vigour of the fermentative processes of acidogenesis and acetogenesis by comparison to methanogenesis, and assuming hydrogen-scavenging methanogens consume all gaseous intermediates (as indicated at 3(ii) above), the stoichiometry and mass balance of the three main steps can be simplified as follows:



In mass terms, the hydrolysis of 1 mol of cellulose (MW = 162g) produces 3 moles carbon dioxide (= 132g) and 3 moles methane (= 48g).

### Kinetics of enzymatic hydrolysis

Unlike in more diffuse aqueous substrates such as sewage sludge, waste refuse is predominantly a solid structured material where the rate and progress of decomposition are constrained by physical factors. In this formulation, modifications have been made to reflect

more realistically the physical factors influencing the solid to aqueous phase transfer. A modified enzymatic hydrolysis function accounts for the influence of moisture content, product inhibition and the changing digestibility of the degradable fraction.

### **Digestibility**

The presence of highly degradable organic matter and/or the initial colonisation and enzymatic attack of exposed waste surfaces mean that initial hydrolysis rates are rapid. Remaining organic matter, having become less accessible to, or shielded from, enzymatic attack, or with an increased crystallinity, becomes less digestible and is hydrolysed at slower rates. Lee & Fan (1982) suggested that a lumped parameter, referred to as the relative digestibility, be used to reflect the combined effects of changes in accessible surface area and crystallinity. They found relative digestibility,  $\phi$ , to be related to the extent of substrate conversion by a single parameter,  $n$ , the structural transformation parameter, i.e.

$$11] \quad \phi = 1 - \left[ \frac{S_o - S}{S_o} \right]^n$$

where  $S$  is the solid organic fraction remaining and  $S_o$  is the initial solid organic fraction.

Lee & Fan reported a value of 0.36 for the structural transformation parameter but indicated that the value is probably strongly dependent on the structural features of the cellulose. In their tests, "Solka-Floc", a commercially available delignified cellulose was used but lignin, a substance which is resistant to enzymatic hydrolysis and can shield cellulose, comprises up to 15% by dry weight of the organic fraction of waste refuse (Bookter & Ham, 1982). Calculations performed on data presented by Wald et al. (1984) for rice straw, a lignified cellulose, reveal a higher value (0.7) for the structural transformation parameter.

### **Product inhibition**

A product inhibition term  $P$ , based on VFA concentration, allows for acid accumulation and associated 'souring' of a site,

$$12] \quad P = \exp(-k_{VFA}(c))$$

where  $k_{VFA}$  is the product inhibition factor and  $c$  is the concentration of volatile fatty acids [units =  $\text{g}_{VFA} \cdot \text{m}^{-3}_{\text{aqueous}}$ ]. Values for  $k_{VFA}$  are chosen to ensure that maximum VFA concentrations correspond to those reported in sites or other installations that are known to have 'soured' or 'stuck'. For the example simulations, a value of  $2 \times 10^{-4} \text{ m}^3/\text{g}$  results in peak VFA values of about  $16,000 \text{ g}/\text{m}^3$ .

### **Maximum rate of hydrolysis**

Denoted by the letter  $b$ , this is the maximum or initial rate of hydrolysis of solid organic matter occurring under the most favourable substrate structure and interaction conditions. The maximum hydrolysis rate determines the accumulation of VFA, principally acetic acid, in the aqueous phase. It has units of mass per unit volume aqueous phase per unit time, i.e.  $\text{g}_{VFA} \cdot \text{m}^{-3}_{\text{aqueous}} \cdot \text{day}^{-1}$ . Estimates of the maximum hydrolysis rate can be made from VFA growth vs. time plots, e.g. from Barlaz et al (1989) wherein a VFA growth rate of about  $1800 \text{ mg}_{VFA} \cdot \text{L}^{-1}_{\text{aqueous}} \cdot \text{day}^{-1}$  can be found. Jones & Grainger (1983) indicate an accumulation of about  $3000 \text{ g}_{VFA} \cdot \text{m}^{-3}_{\text{aqueous}} \cdot \text{day}^{-1}$ .

Alternatively, the loss of solids may be considered. Cecchi et al (1988) and Wang & Banks (2000) indicate maximum volatile solid (VS) reduction rates in the range  $4000\text{g}$  to  $5000 \text{ g}_{\text{totalVS}} \cdot \text{m}^{-3}_{\text{aqueous}} \cdot \text{day}^{-1}$ . It is important to note here that the difference in molecular weights between cellulose or glucose and VFA, means that the solids reduction and VFA accumulation data above are more consistent than they appear. This matter is discussed in more detail in the section on Substrate Depletion, below. That said, work on small in vitro samples of cellulose by Lee & Fan (1983) and more recently by Rodriguez (2005) indicate that laboratory determined values of the maximum hydrolysis of shredded waste are considerably higher.

For the example simulations, a value of  $2500 \text{ mg}_{VFA} \cdot \text{L}^{-1}_{\text{aqueous}} \cdot \text{day}^{-1}$  has been selected.

### **Moisture content**

One of the most important influences on the biodegradation of landfilled waste, and one that can be controlled most easily during the life of a landfill, is moisture. Moisture content and

flow, act as means by which chemical substances and microbes penetrate the waste mass and as a pre-requisite for microbial function. An effective moisture content term based on existing hydraulic properties has been adopted to approximate the influence of moisture on the biodegradation process,

$$13] \quad \theta_E = \frac{\theta - \theta_R}{\theta_S - \theta_R}$$

where  $\theta$  is volumetric moisture content and subscripts  $E$ ,  $S$  &  $R$  refer to effective, saturated and residual respectively.

### **Modified functional form**

Combining the maximum hydrolysis rate with the limiting factors described by Equations [11], [12] and [13] gives an equation describing the enzymatic hydrolysis of waste refuse under a range of moisture contents,

$$14] \quad \begin{aligned} \theta_E r_g &= \theta_E b \phi^P \\ &= \theta_E b \left[ 1 - \left[ \frac{S_O - S}{S_O} \right]^n \right] \exp(-k_{VFA}(c)) \end{aligned}$$

### **Methanogenesis**

The depletion of the methanogenic substrate and methanogen growth are described by Monod kinetics, hence for MB accumulation ( $r_j$ ),

$$15] \quad r_j = \frac{k_0 c}{(k_{MC} + c)} m$$

where  $k_0$  is the maximum specific growth rate,  $k_{MC}$  is the half saturation constant and  $m$  is the MB concentration. The rate of VFA depletion,  $r_h$ , is directly related to MB accumulation through a cell/substrate yield coefficient,  $Y$ ,

$$16] \quad r_h = \frac{r_j}{Y}$$

The MB decay  $r_k$  is given by,

$$17] \quad r_k = k_2 m$$

where  $k_2$  is the methanogen death rate.

Estimates for the methanogenic parameters were originally sought from a literature review but there was little data relating to MSW, and that which was available covered a range of values (see below). These data provided the starting point for methanogenesis parameter selection and were subsequently refined following a parametric sensitivity study (McDougall & Philp, 2001).

Reference	$k_0$	$K_{MC}$	$Y$	$k_2$
Straub & Lynch (1982) Model waste	0.03 day <sup>-1</sup>	5000 mg/L	0.04	0.01 day <sup>-1</sup>
Lee & Donaldson (1985) Cellulose	0.5 day <sup>-1</sup>	4200 mg/L	0.75	0.02 day <sup>-1</sup>
Viturtia (1995) Pig manure	0.57 day <sup>-1</sup>	3280 mg/L	0.19	
El-Fadel (1996) Various	0.25 day <sup>-1</sup>	500 mg/L	0.06	0.03 day <sup>-1</sup>

## Transport, growth and decay - governing equations

The combined transport, growth and decay of VFA and methanogenic biomass in the biodegradation model are defined by,

$$18a) \quad D_c \frac{\partial^2 c}{\partial z^2} - \frac{q}{\theta} \frac{\partial c}{\partial z} + [\theta_E r_g - r_h] = \frac{\partial c}{\partial t}$$

where  $D_c$  is the VFA diffusion coefficient and  $q$  is the advective flux; and,

$$18b) \quad D_m \frac{\partial^2 m}{\partial z^2} - \frac{q}{\theta} \frac{\partial m}{\partial z} + [r_j - r_k] = \frac{\partial m}{\partial t}$$

where  $D_m$  is the methanogenic biomass diffusion coefficient.

Expansion of the growth and decay terms reveals the nature of the interdependency – two simultaneous partial differential equations, which are solved iteratively, by updating system parameters until a consistent solution is obtained.

$$19a) \quad D_c \frac{\partial^2 c}{\partial z^2} - \frac{q}{\theta} \frac{\partial c}{\partial z} + \theta_E b \left[ 1 - \left( \frac{S_0 - S}{S_0} \right)^n \right] \exp(-k_{VFA}(c)) - \frac{k_0 c}{(k_{MC} + c)} \frac{m}{Y} = \frac{\partial c}{\partial t}$$

$$19b) \quad D_m \frac{\partial^2 m}{\partial z^2} - \frac{q}{\theta} \frac{\partial m}{\partial z} + \left[ \frac{k_0 c}{(k_{MC} + c)} m - k_2 m \right] = \frac{\partial m}{\partial t}$$

## Substrate depletion

Solid organic depletion, which is directly related to the accumulation of VFA in the aqueous phase, is determined at the end of each time step. The calculation is based on the modified enzymatic hydrolysis function, which has been modified to account for the transfer of

substances between different phases. There are both volumetric and mass considerations to be considered here.

- a) Reference volumes – the solid degradable content of a landfill is conveniently reported as a mass per unit total volume whereas VFA concentrated in landfill leachate is given as a mass per unit aqueous phase volume. The modified enzymatic hydrolysis function is therefore multiplied by the volumetric moisture content to translate the VFA aqueous phase concentration increase into a loss of solid mass per unit total volume.
- b) The solid organic matter lost is taken to be that of cellulose ( $C_6H_{10}O_5$ ), which has a molecular weight of 162 g/mol, whereas the accumulated VFA is assumed to be principally acetic acid ( $CH_3COOH$ ), which has a molecular weight of 60 g/mol. Therefore, the accumulation of 60g of acetic acid is a result of the solubilisation of 162g of cellulose. A mass conversion factor must therefore be applied to the enzymatic hydrolysis function so that the correct amount of cellulose is depleted per unit increase of VFA mass.

Substrate depletion is thus calculated from,

$$20] \quad S^{t+\Delta t} = S^t - \theta \cdot \frac{162}{60} \theta_E b \phi P \Delta t$$

where  $S_t$  is the SDF remaining at the beginning of the current time step,  $t$ , and  $\Delta t$  is the time step interval.

### Moisture consumption

Consumption of water can be determined from the depleted substrate as follows.

$$21] \quad dM_{H_2O} = \frac{18}{162} dM_{cellulose}$$

---

where  $M$  is the mass of water and cellulose as subscripted and the factor 18/162 is the ratio of the molecular weights of the two substances. Since both volume of moisture and the mass of cellulose are reported to total volume bases, Equation [19] can be divided through by total volume,  $V_T$ , from which is obtained,

$$22] \quad d\theta = \frac{18}{162\rho_{H_2O}} dS$$

Equation [22] defines the consumption of water as a reactant in the hydrolysis process. Reductions in moisture contents due to decomposition are handled as local Neumann boundary conditions in the hydraulic model and are a constraint on the rate of hydrolysis, working through the effective moisture content term.

As already indicated, the direct conversion of cellulose to acetic acid implies that acidogenesis and acetogenesis are robust and rapid processes. This means that in the early stages of landfill biodegradation, acetic acid will accumulate, at least until methanogenesis is established, whereupon hydrolysis becomes the rate-limiting step. Such behaviour has been described many times (e.g. Vavilin et al, 2003).

## Mechanical Model

The mechanical model combines load, creep and biodegradation-induced effects to predict landfill settlement. Applied loads trigger an immediate elastic or elastoplastic settlement, whereas time-dependent creep and rate-limited biodegradation give rise to long-term settlement. Total settlement can be written as the sum of four main strain components,

$$23] \quad \varepsilon_{total} = \varepsilon_e + \varepsilon_p + \varepsilon_c + \varepsilon_b$$

where  $\varepsilon$  is strain and subscripts  $e$ ,  $p$ ,  $c$  and  $b$  denote elastic, plastic, time-dependent creep and biodegradation induced strains respectively.

## PARAMETER REQUIREMENTS

Parameter requirements are given in the table below; justification for the selection of hydraulic parameter values are given in the relevant sections.

	Input parameter	Dimensions	Waste
<b>Mechanical</b>			
M1	Elastic stiffness		0.072
M2	Elastoplastic stiffness		0.23
M3	Poisson's ratio		0.35
I4	Initial yield stress	kPa	30
M4	Creep viscosity		0.0015
M5	Decomposition-induced void		-0.65
M6	Decomposition hardening	kPa	2
I5	Dry unit weight (as placed)	kN.m <sup>-3</sup>	5
M7	Inert phase particle weight	kN.m <sup>-3</sup>	17
M8	Degradable phase particle weight	kN.m <sup>-3</sup>	7.3

## LANDFILL SETTLEMENT

The five landfill settlement mechanisms: mechanical, ravelling, physico-chemical, biochemical, and interaction, first put forward by Sowers (1973), are now well-known. They are difficult to distinguish individually so are usually interpreted using a three-part temporal classification of initial, primary and secondary settlement stages (Morris & Woods, 1990). However, the interpretation of secondary landfill settlement as a time-dependent process is an expediency which masks the fundamental nature of the biodegradation process. We will therefore consider landfill settlement as a combination of separate load, creep and biodegradation settlement processes (McDougall & Pyrah, 2001; 2003)

### Load-induced behaviour - Elasto-plasticity

Load-induced settlement is usually depicted by a compression coefficient or constrained modulus (e.g. Sowers, 1973; Morris & Woods, 1990; Watts & Charles, 1999). This approach may be adequate for short term monotonic settlement, e.g. during infilling, but it is both intuitive and evident that there will be significant plastic compression. Evidence of plastic compression can be obtained from various sources. For example, Kavazanjian et al (1999) measured the compression of reconstituted waste samples in large scale oedometers, shown in Figure 10, from which a clear and consistent difference in elasto-plastic virgin loading and elastic unloading compression coefficients can be observed. Similarly, pressure against

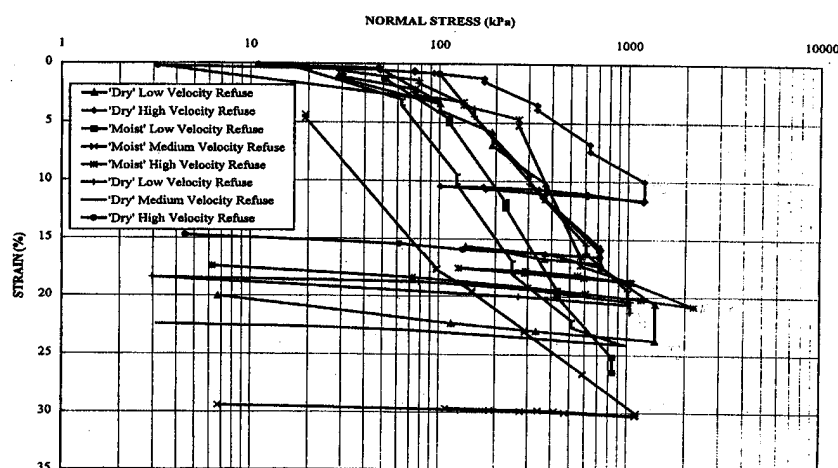
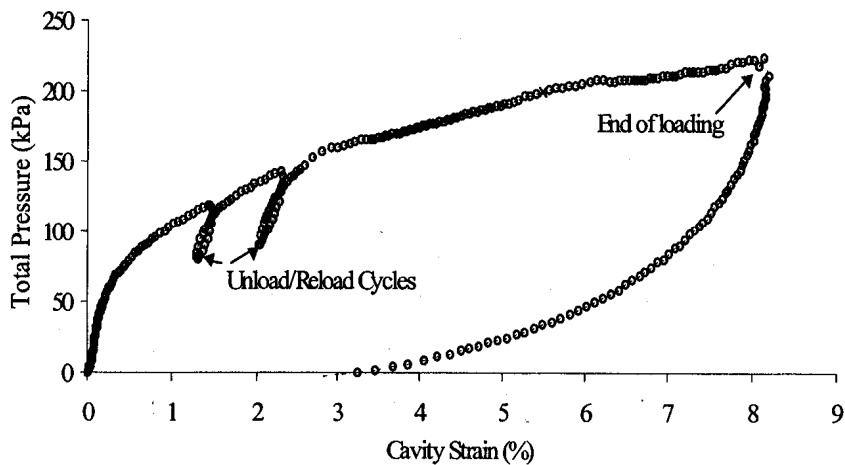


Figure 10. Oedometer test results on waste, reproduced from Kavazanjian, Matasovic & Bacchus (1999)



**Figure 11. Pressure with cavity strain results obtained from in-situ pressuremeter tests, Dixon, Jones & Whittle (1999)**

cavity strain measurements, obtained by Dixon et al (1999) from self-boring pressuremeter tests in a relatively young waste, presented in Figure 11, show elasto-plastic virgin compression with elastic unload-reload behaviour.

In the HBM model, load-induced compression is handled using a simplified version of an elastoplastic geomechanical model (Modified Cam Clay). The following paragraph is included introduces some of the key features of such an approach.

### ***Elastoplasticity: key features***

The concept of an elastoplastic geomechanical model means that waste compression responds to load in the context of a yield stress. If the current loading state is less than a predetermined yield stress then settlement is elastic and relatively small in magnitude. This kind of behaviour would be anticipated when newly placed and compacted waste is first loaded. At higher loadings, when the yield condition is met, settlement is relatively large. Modified Cam Clay depicts a volumetric hardening material, which means that plastic volumetric strains increase the yield stress. The practical impact of an increased yield stress is most apparent during if virgin (or elastoplastic) loading is followed by an unload-reload cycle. The virgin loading produces relatively large compressive strains and marks a maximum loading condition known as the preconsolidation pressure. Subsequent unloading

is elastic, as is reloading, regardless of the loading stress path followed. However, once the preconsolidation pressure is reached, compression becomes elastoplastic. It is as if the soil remembers its loading history and on reaching the preconsolidation pressure (or more general yield condition), switches from a relatively predictable elastic zone into a more responsive elastoplastic mode.

### Creep behaviour - Visco-elasto-plasticity

Creep behaviour in an inert soil, due to time-dependent particle deformation and/or slippage at particle contacts, was described by Bjerrum (1967), in conjunction with elasto-plastic load-induced compression. He noted, during periods of constant loading, the development of a reserve resistance to additional loading; in other words, creep settlement produces an increase in the effective preconsolidation pressure, thereby creating a stage of relatively stiff, elastic straining before elasto-plastic virgin compression is regained. In a series of laboratory experiments, Landva et al (2000) applied an alternating vertical stress increment and creep loading path to a 9 year old partly decomposed waste in large (450mm) oedometers. Each of the creep loading stages lasted for a period of one week only so none allowed for much (if any) biodegradation. Their results, reproduced in Figure 12, clearly indicate a form of visco-elasto-plastic settlement behaviour identical to that proposed by Bjerrum for more conventional soils.

Yin & Graham (1989) proposed an equivalent time method for the analysis of both creep deformation and changes in loading. Based on the Bjerrum approach, is well suited to an elastoplastic framework but only developed for one-dimensional deformation. Figure 13 shows an idealized oedometric stepped loading sequence with the corresponding time:loading history and notation.

Consider the loading condition depicted by point 6'. Yin and Graham show that creep deformation from this point is given by,

$$24] \quad \varepsilon_c = \Psi \ln \left[ \frac{t - t_{c=2} + t_{eq,c=3} + t_{ref}}{t_{ref}} \right]$$

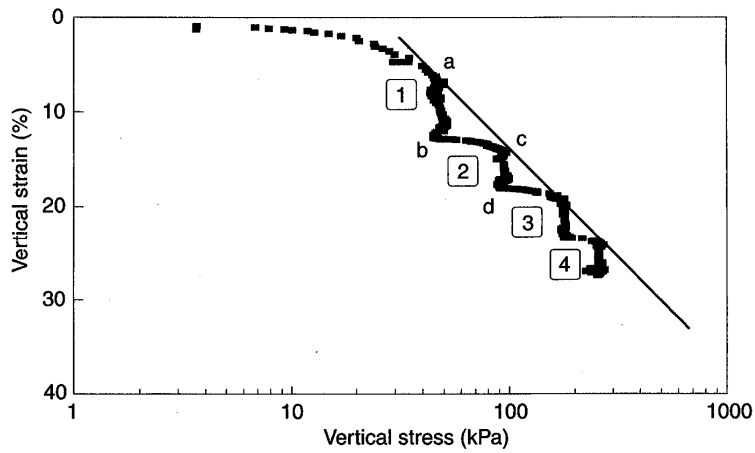


**Figure 12. Creep behaviour of waste refuse; reproduced from Landva et (2000).**

where  $\Psi$  is here the creep viscosity coefficient,  $t$  is the current time,  $t_{c=2}$  is the time at the end of the second (previous) creep stage, which equals the beginning of the current creep stage assuming instantaneous load response,  $t_{eq, c=3}$  is the equivalent time for the current creep stage, and  $t_{ref}$  is a reference time, which is here assumed to be equal to 1 day.

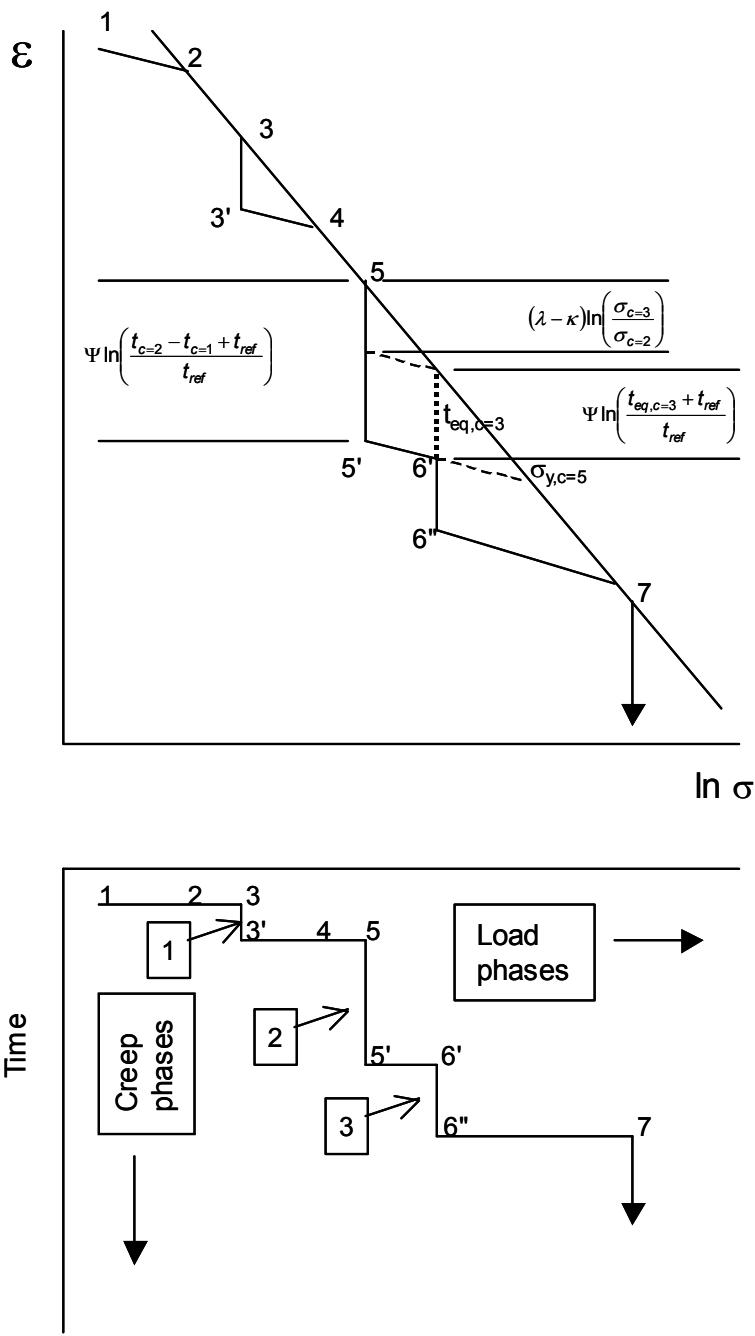


Figure 13. Idealised stepped loading and creep sequence with associated strain response.

## Biodegradation-induced settlement: Bio-plasticity

The progress of biodegradation is known to contribute significantly to the magnitude of secondary settlement in landfills. However, its dependence on biochemical entities, such as leachate characteristics and microbial activity, means it is difficult to integrate meaningfully into time-dependent analyses of secondary settlement.

There are, however, a number of laboratory and field scale data sets on the settlement behaviour of 'non-conservative' (decomposing) soils and landfilled waste, from which it is possible to deduce something of the mechanical consequences of decomposition. A review of this data (McDougall et al, 2004) highlights observed behaviour and the consequences of changes in phase composition in degradable materials. Consider Figure 14 for example, which shows layer strains in a 3 year old highly organic waste at the Muribeca Landfill site in Brazil. At depths of 18m and less, layer strain curves show periods of zero strain or even apparent layer expansion and subsequent collapse.

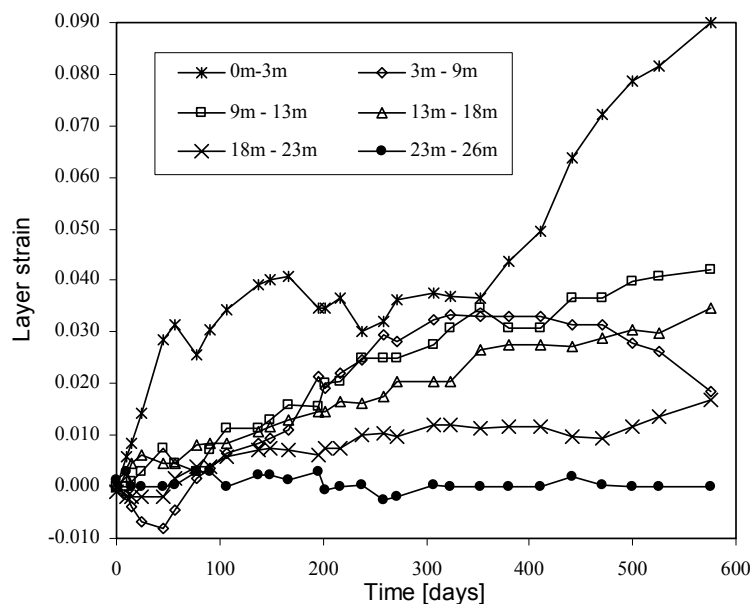


Figure 14. . Individual layer strain in landfilled waste at Muribeca, reproduced from McDougall et al (2004).

The treatment of biodegradation settlement in the HBM model differs from more conventional soil mechanics approaches by the inclusion of a constitutive relationship between decomposition of solid degradable fraction, in other words between a change in solid phase volume  $V_S$ , and the induced change in void volume  $V_V$ , i.e.

$$25] \quad dV_V = \Lambda dV_S$$

where  $\Lambda$  is the decomposition-induced void change parameter.

There are two important consequences of this approach. Firstly, biodegradation settlement is not treated as a simple time-dependent process. Time is communicated through solid organic matter depletion, which is controlled by the biodegradation model. In this way there is a maximum rate of depletion but within that rate, under the influence of acid accumulation or a moisture deficit/addition for example, decomposition may slow down, accelerate, or stop completely. Table 2 summarises the mechanical response to decomposition, in terms of both volume and strength, for certain key values of  $\Lambda$ . A full description and derivation of  $\Lambda$  can be found in McDougall & Pyrah, 2004.

$d\Lambda$	Void inert ratio	Void ratio	Mechanical consequences
$d\Lambda \gg e$	Decreasing Significantly	Decreasing	Collapse
$d\Lambda = e$	Decreasing	Constant	Contemporaneous Rearrangement
$d\Lambda = 0$	Constant	Increasing	
$d\Lambda = -1$	Increasing	Increasing Significantly	Pure void enlargement

Secondly, this approach allows for the definition of hardening or (more likely) softening with decomposition. Notice in the table that  $\Lambda = e$  is particularly significant. When  $\Lambda < e$  the void ratio increases and by implication the material becomes weaker, whereas when  $\Lambda > e$  the void ratio decreases implying a strength increase. A biodegradation hardening rule can therefore be defined,

$$26] \quad d\sigma_y = \Omega \frac{(e - \Lambda)}{V_s} dV_s$$

where  $\Omega$  is a multiplier that relates the magnitude of increments of yield stress to increments of strain. The qualitative behaviour of the yield condition and its response to the biodegradation hardening rule is shown in Fig. 15. When  $\Lambda < e$ , reductions in solid volume are associated with reductions in yield stress, i.e. the material softens. In contrast, when  $\Lambda > e$ , reductions in solid volume produce an increase in yield stress and the material hardens.

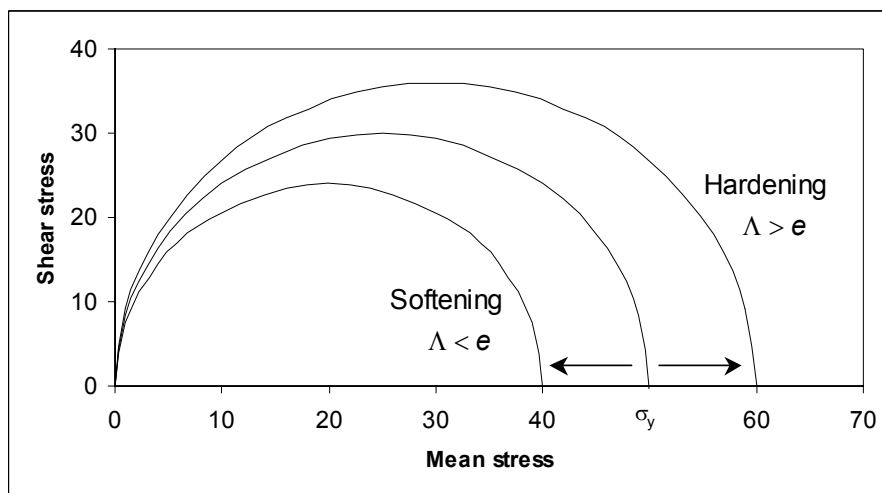


Figure 15. Changes in position of yield surface with decomposition

## PARAMETER ESTIMATION – LABORATORY TESTS

A waste compression, decomposition and settlement test was performed in the LIRIGM laboratories at University of Grenoble (Olivier et al., 2003). The test was a run for a period of 677 days under a vertical stress of 130 kPa. The experiment was performed on 575 kg of wet waste placed in a cell of approximately 1 m<sup>2</sup> plan area, to a depth of 0.845 m. The waste had an overall bulk unit weight of 6.81 kN/m<sup>3</sup>, dry unit weight of 4.28 kN/m<sup>3</sup>, a gravimetric moisture content of 59%, and a degradable:inert mass ratio of 55:45.

A back analysis of the settlement data was performed using the HBM model (McDougall & Hay, 2005). A mesh comprising four quadrilateral elements corresponding to each of the fill lifts was used.

The mechanical analysis enabled best fit values for compressibility parameters ( $\lambda = 0.23$ ,  $\kappa = 0.072$ ,  $\nu = 0.35$ ), creep viscosity parameter ( $\psi = 0.0015$ ), and initial yield stress (30kPa) to be determined. Indeed, no difficulty was anticipated in obtaining a good fit to the initial data for a simple loading and creep condition. However, further extension of the loading ram produced an unload-reload sequence at about 70 hours, which defines more tightly the choice of load and creep parameters, the results of which can be seen in Fig.16.

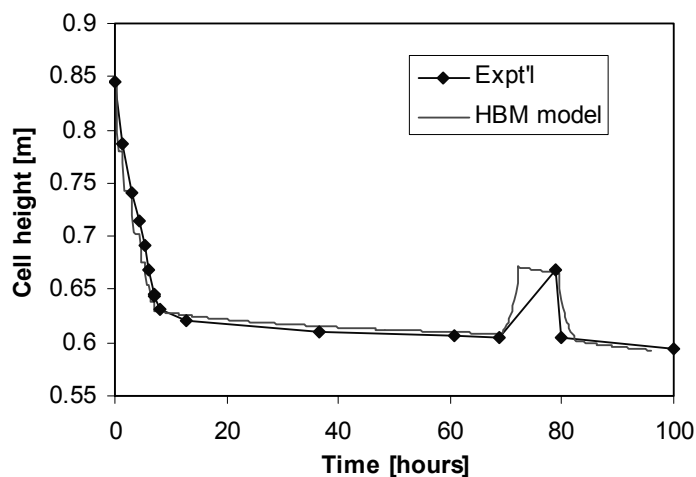


**Figure 16. Laboratory data (Olivier et al, 2003) and HBM model results over initial loading phase**

The next part of the simulation aimed to capture the secondary settlement over the full 677 days. No further changes in mechanical compressibility or viscosity parameters were allowed. However, it is necessary to set a value for the decomposition-induced volume change parameter,  $\Lambda$ .

The results shown in Fig.17 show long-term settlement for selected values of  $\Lambda$ . Best fit, particularly to the acceleration in settlement at about 300 days, occurs with  $\Lambda \approx -0.65$ . Such values of  $\Lambda$  correspond to a loosening of the waste with decomposition. A further check on

performance can be made by comparison of the measured and predicted loss of solid mass, which is the subject of ongoing investigations.

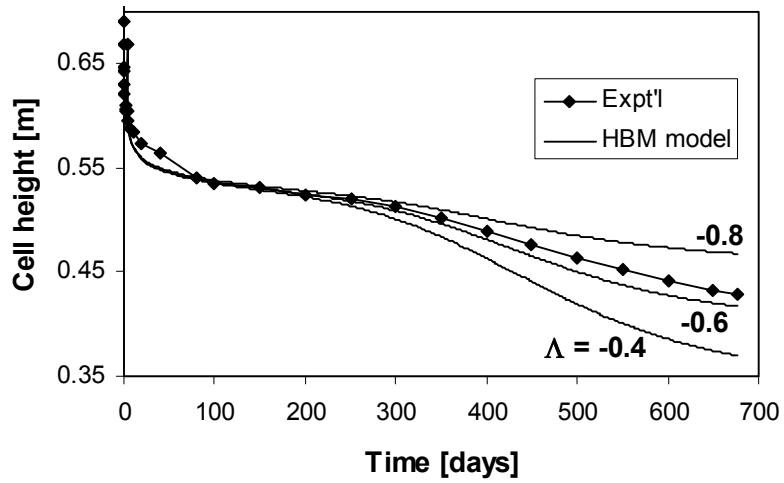


Figure 17. Laboratory data (Olivier et al, 2003) and HBM model results for secondary settlement

## Initial conditions

### HYDRAULIC VARIABLES

An essential part of any simulation is the determination of the initial phase composition, both weights and volumes. Dry density data in conjunction with inert and degradable fractions and phase weights (specific gravities) fix the dry weights, solid and void volumes. However, in order to obtain physically consistent pressure head and moisture content data it is necessary to initialise the hydraulic system. The GUI is configured to simplify the initialisation of the hydraulic system but it may require several adjustments to the hydraulic boundary conditions in order to create the required moisture content distribution. The procedure is important, however, since physically inconsistent or implausible initial hydraulic conditions will undermine the transient analysis.

### BIODEGRADATION VARIABLES

The initial values of biodegradation variables, VFA and MB concentrations, are specified inputs. The suggested values have been guided by a parametric sensitivity analysis (McDougall & Philp, 2001).

### VFA

The enzymatic hydrolysis process is so vigorous that the initial VFA concentration has virtually no influence over long term concentrations and biodegradation, see Fig.18.

### Methanogenic biomass

In contrast, the slow accumulation of MB means that initial concentrations influence VFA accumulation and conversion over a relatively long time period.

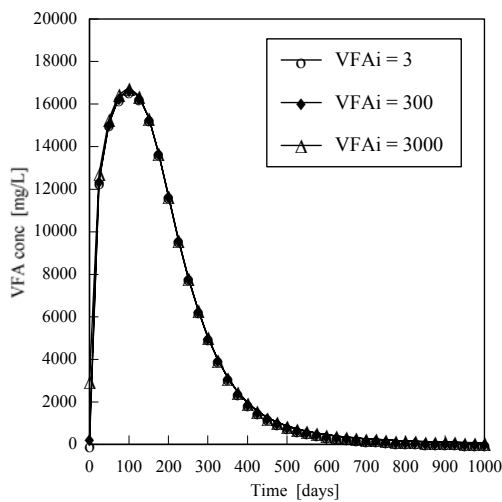


**Figure 19. Sensitivity of VFA concentration to initial values (VFAi). All values given in  $\text{g/m}^3$ , taken from McDougall & Philp (2001)**

Figure 19 shows the earlier and lower peak VFA concentrations due to higher initial MB concentrations together with the associated SDF depletion curves. It would appear that high MB concentrations are not essential for SDF depletion, but when present as an initial stock, they do accelerate the onset of methanogenesis.

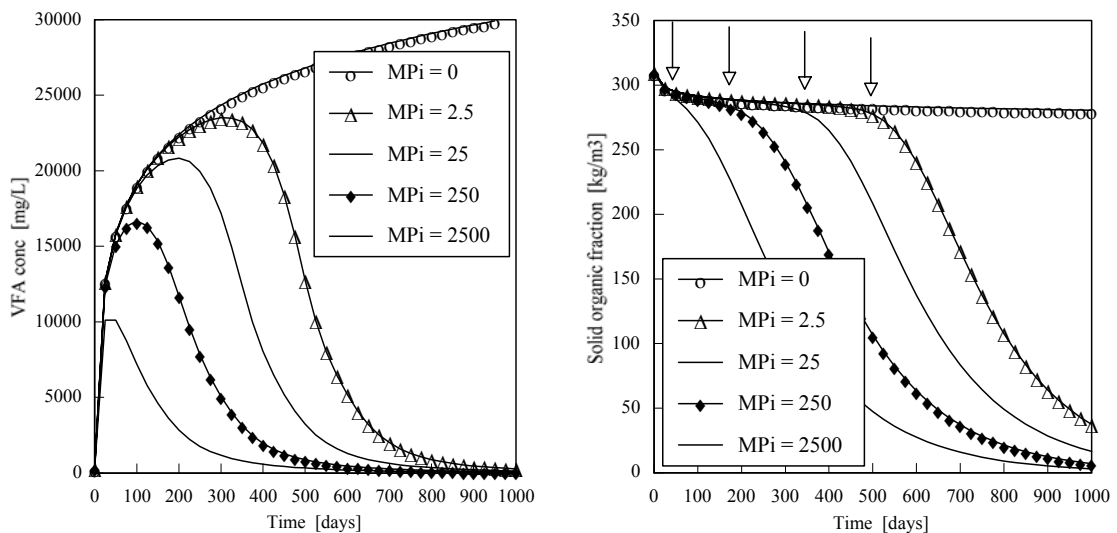


**Figure 18: Sensitivity of MB concentration (left) and SDF (right) to initial values (MBi). All values given in  $\text{g/m}^3$ , taken from McDougall & Philp (2001)**

## Link Routines

The HBM algorithm guides the solution between system models via link routines. These link routines contain calculation procedures by which system parameters and other derived data, principally phase composition data, are updated according to the most recent system variable values. The procedures executed by each link routine are given below.

### HYDRAULIC-BIODEGRADATION (HB) LINK

Updated volumetric moisture content data is available on exit from the hydraulic model. The HB link routine recalculates moisture volumes, gas volumes, element water weight, element total weight, degree of saturation and other phase ratios.

### BIODEGRADATION-MECHANICAL (BM) LINK

The biodegradation model determines solid phase depletion and mass remaining. The BM link routine firstly calculates new solid weight, total weight and gravimetric moisture content. After calculation of solid phase volume loss, induced void phase volume change is determined using  $\Delta$ ; all associated phase volumes, ratios, and derived parameters such as unit weights are then updated. The mechanical yield stress is updated in this routine.

### MECHANICAL-HYDRAULIC (MH) LINK

The mechanical model determines compression of each element due to reductions in void volume. Once void and total volumes are updated, all phase ratios and derived parameters are adjusted. Saturated hydraulic conductivity, if density-dependent, is adjusted here.

In this routine the physical hydraulic parameters, the residual moisture content and saturated moisture content are updated in preparation for the ensuing hydraulic system solution. Note that density and porosity data are defined over the elements of the finite element mesh, whereas moisture contents are defined at mesh nodes. A mechanism for allocating distributed element properties to the nodal points is an essential part of each link routine.

---

## Element types

The HBM model can use both three-noded triangular and four-noded isoparametric quadrilateral (or serendipity) elements. The triangular elements are not used in the current simulations.

Whilst the limitations of lower order elements are widely recognised for numerical analysis of mechanical problems, a number of factors have postponed moves towards the introduction of higher order elements. These factors are:

- **Hydraulic.** The steady state condition (either hydrostatic or infiltrative) results in a linear variation in the field variable, the hydraulic pressure head. It is unclear at this stage whether transient effects, such as pronounced variations in pressure head around wetting fronts, are better handled with higher order elements or local mesh refinement.
- **Biodegradation.** The principal output of the biodegradation model is the depletion of the solid organic fraction. The strength of enzymatic hydrolysis and methanogen growth terms in the evolution of VFA and MB concentrations compared with the diffusive and advective transport terms reduces the significance of the order of the element shape function.
- **Mechanical.** The significance of biodegradation in the long-term settlement behaviour of waste and, more importantly, its interpretation within a landfill settlement model, has been a greater priority than the prediction of stress states within the waste mass.

So, without any pressing need to introduce higher order elements and recognising the fact that numerical implementation of the HBM model has had to be coded completely 'from scratch', recent development of the model has relied solely on the four-noded isoparametric quads.

---

## Numerical control

Solutions for the hydraulic and biodegradation system equations are obtained using a Gauss-Seidel iterative solver, the stability of which is dependent on a number of controlling parameters. Default values, drawn from many sensitivity analyses, are given below. Solution accuracy may be improved by control of these parameters but such changes should not be attempted without some knowledge of their form and influence.

### **Over-relaxation parameter, $\omega$**

Accelerates the rate of convergence of the Gauss-Seidel solver by over-estimating (assuming values  $> 1.0$ ) the initial values adopted in the next iteration.

### **Time step predictor, $\kappa$**

The predictor in a predictor-corrector method of time-stepping. In a non-linear system of equations, material parameters depend on the field variable. In a transient analysis, the material parameters must be consistent with the advancing solution at all stages of the simulation. The predictor controls the amount by which the current solution is adjusted to provide a better estimate of the material parameters on entry into the next time step.

### **Time step corrector, $\lambda$**

It is common that the predictor step described above, on entry to a new time step, does not lead to a solution that is consistent with the predicted material properties. The corrector term allows for further adjustment of the solution upon which the material properties are calculated within the new time step. The influence of  $\lambda$  is evident as the number of calculation updates required in either the hydraulic and/or biodegradation systems.

### **Time stepping recursion parameter, $\theta_h$**

The time stepping recursion parameter controls the finite difference time discretisation of the hydraulic and biodegradation models. In the hydraulic model, the formulation of the governing equations results in a capacitance matrix which, under saturated conditions, becomes zero. Assigning a value of 1.0 to the recursion parameter  $\theta_h$  results in a backward difference approximation and avoids the solution being dependent on an undefined matrix.

**Time stepping recursion parameter,  $\theta_b$** 

The same form of time discretisation is employed in the biodegradation model. For consistency,  $\theta_b$  has also been assigned a value of 1.0.

Parameter	Value
$\Omega$	1.2
$\kappa$	0.4
$\lambda$	0.4
$\theta_h$	1
$\theta_b$	1

---

## References

- Barlaz M.A., Ham R.K. & Schaefer D.M. (1989) Mass balance analysis of anaerobically decomposed refuse. *A.S.C.E., J. Env. Eng. Div*, 115, 6, 1088-1102.
- Beaven, R.P. (2000) The hydrogeological and geotechnical properties of household waste in relation to sustainable landfilling. *PhD Thesis, Queen Mary and Westfield College, University of London*
- Bookter T.J. & Ham R.K. (1982) Stabilization of solid waste in landfills. *A.S.C.E., J. Env. Eng. Div*, 108, EE6, 1089-1100.
- Bjerrum L. (1967) Engineering geology of normally consolidated marine clays as related to the settlement of buildings. *Geotechnique*, Vol 17, No.2., 83-118
- Cecchi F., Traverso, P.G., Claney, J. & Zaror, C. (1988) State of the art of R&D in the anaerobic digestion process of municipal solid waste in Europe. *Biomass*, 16, 257-284.
- Dixon N., Jones D.R.V. & Whittle R.W. (1999) Mechanical properties of household waste: In situ assessment using pressuremeters. *Proceedings Sardinia '99, Seventh International Waste Management and Landfill Symposium*, CISA, Cagliari, Vol 3, 453-460
- El-Fadel, M, Findikakis, A.N. & Leckie, J.O. (1996) Numerical modelling of generation and transport of gas and heat in landfills I. Model formulation. *Waste Man. & Res.* Vol.14. 483-504.
- Jones, K.L. & Grainger, J.M. (1983) The application of enzyme activity measurements to a study of factors affecting protein, starch and cellulose fermentation in domestic refuse. *European J. Appl. Microbiology & Biotech.*, Vol.18. 181-185.
- Kazimoglu, Y.K., McDougall, J.R. & I.C.Pyrah (2005) Moisture retention and movement in landfilled waste. *Proc. GeoProb2005. Int'l. Conf. on Problematic Soils*, Eastern Mediterranean University, North Cyprus, May 2005, ed. Bilsel, H. pp 307-314
- Kavazanjian E., Matasovic N. & Bachus R. (1999) Large-diameter static and dynamic testing of municipal solid waste. *Proceedings Sardinia '99, Seventh International Waste Management and Landfill Symposium*, Vol 3, 437-445.
- Landva A.O., Valsangar A.J. & Pelkey S.G. (2000) Lateral earth pressure at rest and compressibility of municipal solid waste. *Canadian Geot. J.*, Vol. 37, 1157-1165
- Lee, D.D. & Donaldson, T.L. (1985) Anaerobic digestion of cellulosic wastes. *Biotechn & Bioeng. Symp* No.15. 549-560.

- 
- Lee Y-H. & Fan L.T. (1982) Kinetic studies of enzymatic hydrolysis of insoluble cellulose: (I) Analysis of the initial rates. *Biotechn. & Bioeng.*, 24, 2383-2406.
- Lee Y-H. & Fan L.T. (1983) Kinetic studies of enzymatic hydrolysis of insoluble cellulose: (II) Analysis of extended hydrolysis times. *Biotechn. & Bioeng.*, 25, 939-966.
- McDougall, J.R. & Philp, J.C. (2001) Parametric study of landfill biodegradation modelling: methanogenesis and initial conditions. *Sardinia 2001, 8th Intl Waste Man. & Landfill Symp*, S.Margherita di Pula, eds. Christensen, Cossu & Stegmann, CISA Cagliari, Vol 1, pp 79-88.
- McDougall, J.R. & Pyrah, I.C. (2001) Settlement in landfilled waste: extending the geotechnical approach. *Sardinia 2001, 8th Intl Waste Man. & Landfill Symp*, S.Margherita di Pula, eds. Christensen, Cossu & Stegmann, CISA Cagliari, Vol 3, pp 481-490.
- McDougall, J.R. & Pyrah, I.C. (2003) Modelling load, creep and biodegradation settlement in landfill. *Sardinia 2003, 9th Intl Waste Man. & Landfill Symp*, S.Margherita di Pula, eds. Christensen, Cossu & Stegmann, CISA Cagliari, CD only.
- McDougall J.R., & Pyrah I.C. (2004). Phase relations for decomposable soils. *Geotechnique*, Vol 54, No7, pp 487-494.
- McDougall J.R., Pyrah I.C. & Yuen S.T.S. (2004) Extended phase relations and load effects in MSW. *Waste Man.* Elsevier Science, Vol 24, 251-257.
- McDougall, J.R., Pyrah, I.C., Yuen, S.T.S., Monteiro, V.E.D., Melo, M.C. & Juca, J.F.T. (2004) Decomposition and settlement in landfilled waste & other soil-like materials. *Geotechnique*, Vol 54, No 9, pp 605-610.
- McDougall, J.R. & Hay, J. (2005) Hydro-bio-mechanical modelling of landfilled waste: formulation and testing. *Proc. Int'l. Workshop on Hydro-Physico-Mechanics of Landfills*, University of Grenoble, March 2005.
- Morris D.V. & Woods C.E. (1990) Settlement and engineering considerations in landfill and final cover design. In *Geotechnics of Waste Fills*, Landva & Knowles (Eds), ASTM STP 1070, Philadelphia, pp 9-21.
- Olivier, F. Gourc, J.P. Lopez, S., Benhamida, S. & Van Wyck, D. (2003). Mechanical behaviour of solid waste in a fully instrumented prototype compression box. *Sardinia 2003, 9th Intl Waste Man. & Landfill Symp*, S.Margherita di Pula, eds. Christensen, Cossu & Stegmann, CISA Cagliari, CD only
- Powrie, W., Richards, D.J. & Beaven, R. (1998) Compression of waste and implications for practice. In *Geotechnical Engineering of Landfills, Proc. Symp. East Midlands Geotechnical Group*, eds. Dixon, Murray & Jones, Thos Telford, 3-18.

- 
- Rodriguez, C (2005) Activité biologique dans les centres d'enfouissement technique de déchets ménagers: biodisponibilité de la cellulose et modélisation. *PhD Thesis, Université de Liège, Centre Wallon de Biologie Industrielle.*
- Sowers G.F. (1973) Settlement of waste disposal fills. *Proc 8th Int'l Conf. Soil Mechanics & Foundation Eng.*, Moscow, ISSMFE, 207-211
- Straub, W.A. & Lynch, D.R. (1982). Models of landfill leaching: moisture flow and inorganic strength. *J. Env. Eng.*, Am. Soc. Civ. Eng. **108**, EE2, 231-250.
- van Genuchten, M.T. 1980 A closed form equation for predicting the hydraulic conductivity of unsaturated soils. *Soil Sc. Soc. of America J.*, Vol.44, pp 892-898.
- Vavilin, V.A., Rytov, S.V., Lokshina, L.Y., Pavlostathis, S.G. & Barlaz, M. (2003) Distributed model of solid waste anaerobic digestion. *Biotech & Bioeng*, Vol. 81, No. 1, 66-73.
- Viturtia, A., Llabres-Luengo, P., Cecchi, F. & Mata-Alvares, J. (1995) Two-phase kinetic model fitting in a two-phase anaerobic digestion of highly biodegradable organic matter. *Env. Technology*, Vol.16. pp379-388.
- Wald S., Wilke C.R. & Blanch H.W. (1984) Kinetics of the enzymatic hydrolysis of cellulose. *Biotechn. & Bioeng.*, 26, 221-230.
- Wang Z. & Banks C.J. (2000) Accelerated hydrolysis and acidification of municipal solid waste in a flushing anaerobic bio-reactor using treated leachate recirculation. *Waste Man. & Res.*, 18, 215-223.
- Watts J.A. & Charles K.S. (1999) Settlement characteristics of landfill wastes. *Geotechnical Eng.*, Vol. 137, No. 4, 225-233.
- Yin & Graham (1989) Viscous-elastic-plastic modelling of one-dimensional time-dependent behaviour of clays. *Canadian Geotechnical J.* 26, pp 199-209.
- Yuen STS. (1999) Bioreactor landfills promoted by leachate recirculation: A full scale study. *PhD Thesis, University of Melbourne, Australia, 1999.*

## Appendix 1 Summary of HBM Parameters

	Input parameter	Dimensions	Waste
<b>Hydraulic</b>			
H1	Van Genuchten $\alpha$		1.4
H2	Van Genuchten $n$		1.6
H3	Residual moisture content (w/w)		0.25
H4	Specific storage		0
H5	Saturated hydraulic conductivity	$\text{m}\cdot\text{s}^{-1}$	$5\times 10^{-5}$
H6	Ratio: vert. to horiz. conductivity		1
<b>Biodegradation</b>			
B1	Maximum hydrolysis rate	$\text{g}\cdot\text{m}^{-3}_{(\text{aq})}\cdot\text{day}^{-1}$	2500
B2	Product inhibition	$\text{m}^3\cdot\text{g}^{-1}$	$2\times 10^{-4}$
B2	Digestibility		0.7
B3	Half rate	$\text{g}\cdot\text{m}^{-3}$	4000
B5	Methanogen growth	$\text{day}^{-1}$	0.02
B6	Methanogen death	$\text{day}^{-1}$	0.002
B7	Yield coefficient		0.08
B8	Diffusion coefficient	$\text{m}^2\cdot\text{day}^{-1}$	0.05
I1	Initial solid degradable fraction		0.4
I2	Initial VFA concentration	$\text{g}\cdot\text{m}^{-3}$	300
I3	Initial methanogenic biomass	$\text{g}\cdot\text{m}^{-3}$	250
<b>Mechanical</b>			
M1	Elastic stiffness		0.072
M2	Elastoplastic stiffness		0.23
M3	Poisson's ratio		0.35
I4	Initial yield stress	kPa	30
M4	Creep viscosity		0.0015
M5	Decomposition-induced void		-0.65
M6	Decomposition hardening	kPa	2
I5	Dry unit weight (as placed)	$\text{kN}\cdot\text{m}^{-3}$	5
M7	Inert phase particle weight	$\text{kN}\cdot\text{m}^{-3}$	17
M8	Degradable phase particle weight	$\text{kN}\cdot\text{m}^{-3}$	7.3